

# DIC ANALYSIS OF CRACK INITIATION AND GROWTH IN THE MODIFIED BRAZILIAN TEST OF STEEL FIBER-REINFORCED CONCRETE

VAIBHAV W. MASIH\*, GONZALO RUIZ<sup>†</sup>, RENA C. YU<sup>‡</sup> AND ANGEL DE LA ROSA<sup>‡</sup>

\*Universidad de Castilla-La Mancha (UCLM)  
Avda. Camilo José Cela s/n, 13071 Ciudad Real, Spain  
e-mail: \* Vaibhavwillson.masih@uclm.es

**Key words:** DIC, Cohesive fracture, Fiber Reinforced Concrete, Composites, Durability

**Abstract.** The Brazilian test is widely used to measure the indirect tensile strength of rocks and concrete. In this study, a Digital Image Correlation (DIC) system is incorporated during the split tensile test to capture and characterize the complex full field deformation, crack nucleation and propagation in steel fiber reinforced concrete (SFRC) specimens, along with the comparison and correlation with the data computed through strain gauges on both faces of the specimen. The displacement and in-plane strain fields are evaluated across the full surface of the specimens using DIC. In the standard practice of Brazilian tests, the computation of matrix failure or load responsible for crack initiation in the concrete matrix is difficult. Using DIC it is possible to capture the exact location of crack initiation and the load corresponding to the crack initiation.

Due to the difficulty of performing a direct uniaxial tensile test, Brazilian tests are used to assess the indirect tensile strength of concrete. The indirect tensile strength is typically calculated based on the assumption that the fracture failure occurs at the point of the maximum tensile stress i.e., at the center of this specimen. To make sure that the width of the loading contact and the stability of the specimen during a test, this research introduces the T-shape loading mechanism along with the hinge arrangement above the specimen. The results show the test's success with no instability of the specimen during the test and crack propagation at the center of the specimen.

## 1 INTRODUCTION

The Brazilian test (BT) is widely employed for the characterization of tensile strength due to its convenient setup for simple compression loading. However, in order to ensure an accurate interpretation of the results and determination of tensile strength, it is imperative to ascertain the initiation location of cracks and analyse the nature of the induced fracture (tensile or shear). This study integrates a 2D-Digital Image Correlation (DIC) system into the BT procedure to effectively capture and analyse the intricate deformation patterns exhibited by SFRC samples [1, 2]. Utilizing DIC, the dis-

placements and in-plane strain fields are comprehensively evaluated across the entire surface of the specimens. The investigation examines the variations in failure load, displacement, strain fields, and final fracture patterns induced by testing as a function of the orientation of bedding planes in relation to the loading axis. Through the implementation of DIC, it becomes possible to precisely identify the sites where fracture initiation occurs, thus facilitating the determination of the validity of each specific experiment for the evaluation of tensile strength. The fractures observed in the reliable tensile test experiments are conclusively classi-

fied as tensile fractures based on the strain fields observed at the locations of crack initiation.

## 2 SPECIMEN PREPARATION AND EXPERIMENTAL SETUP

### 2.1 Material

Material proportions are arrayed in Table 1. The compressive strength obtained with 150 mm  $\times$  300 mm (diameter  $\times$  height) cylinders was  $56.7 \pm 1.8$  MPa (average  $\pm$  std. dev.), whereas it reached  $58.6 \pm 3.4$  MPa when measured with 100 mm  $\times$  100 mm cubes. The elastic modulus was  $32.9 \pm 0.8$  GPa.

Table 1: Material proportions

Raw material	[kg/m <sup>3</sup> ]
Cement	380
Water	182
Superplasticizer	3.800
Air Occluded reducer	1.518
Limestone Powder	90
Fine Aggregate 0/4mm	950
Coarse Aggregate 4/12 mm	525
Coarse Aggregate 12/20 mm	225
Steel Fiber	47.1

### 2.2 Modified Brazilian Test

Numerous standardized methods exist for conducting the BTS (Brazilian Tensile Strength) test to measure tensile strength. The most commonly employed approaches are the ISRM and ASTM methods, which define both direct and indirect Brazilian test methods.

Traditionally, the BTS test involved flat loading platens. However, recent research suggests that curved platens might be more suitable to alleviate the crushing effect at loaded points. It has been observed that the elastic properties of the material remain unaffected by the loading configuration [2], but curved loading platens are difficult to stabilize the test control [3], and it also constrains the specimen geometrical shape to be cylindrical, whereas in case of SFRC, cubic specimens are best to test due to the proper fiber orientation in the specimen.

Therefore, the testing specimen in this experimental program is a cubic specimen of size 100 mm. The tests were performed by applying a compressive load at two points using a T-shaped loading device cushioned with two 3D-printed plastic fillers of a very low elastic modulus (about 0.1% of that of concrete), along with a hinge mounted on top of it, specifically designed to minimize the load eccentricity. The configuration of the test setup is schematically shown in Fig. 1a. The bearing width of the T is 15% the cube side ( $b/L = 0.15$ ), which represents a reasonable compromise between the stability of the set-up and the desired profile of tensile stresses in the cube, see Fig. 1b. A 1 MN servohydraulic universal testing machine (Instron 8801) was utilized at the Materials and Structures Laboratory of the Civil Engineering School of the University of Castilla-La Mancha in Ciudad Real, Spain.

### 2.3 Image Acquisition by Digital Image Correlation (DIC)

#### 2.3.1 DIC Setup & Specimen Preparation

In the realm of material deformation measurement, DIC emerges as a sturdy non-contact technique [4–6]. By utilizing image registration algorithms, DIC adeptly tracks relative displacements between material points in a reference (typically undeformed) image and a current (typically deformed) image [7,8]. Its versatility knows no bounds, allowing for deformation analysis across various scales, from meters to the nanoscale [9–10], as long as the material is suitably patterned and imaged. Over the years, DIC has been successfully applied to study the behavior of diverse systems, ranging from biological materials, metal alloys, shape memory alloys, porous metals, polymers, to polymer foams [11]. Nevertheless, certain material systems present unique challenges, necessitating adaptations to standard DIC algorithms, especially in scenarios of highly localized deformation or significant strains.

In pursuit of accurate full-field measurements, the efficacy of DIC software algorithms

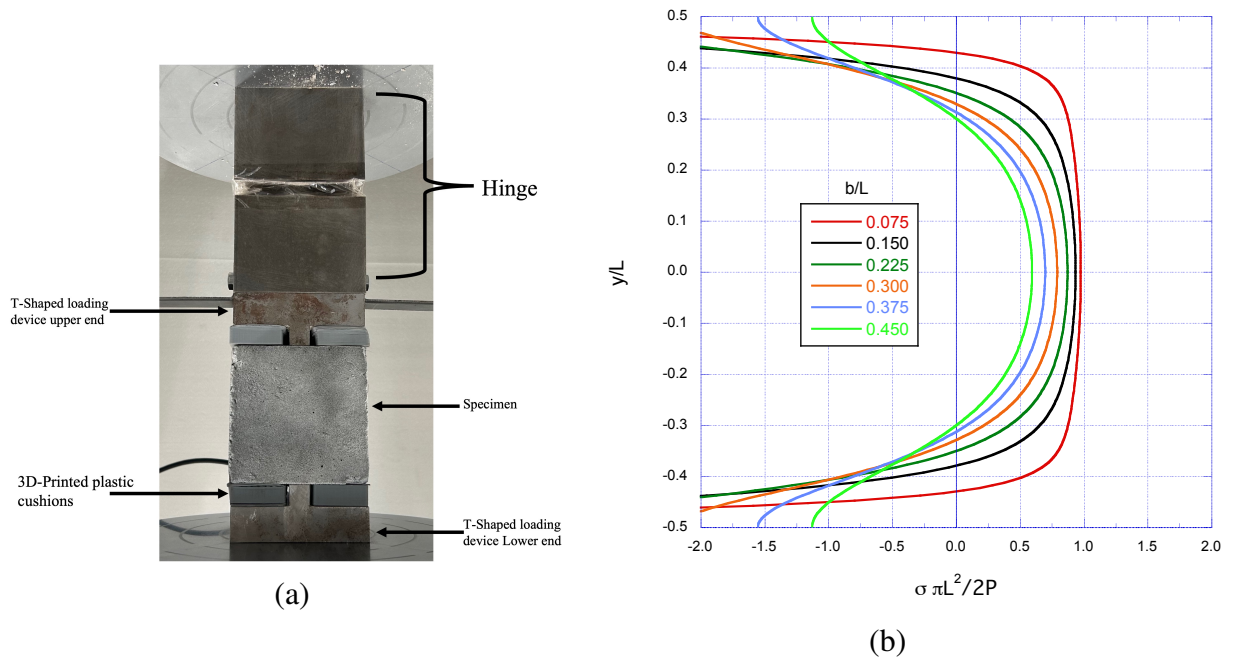


Figure 1: a) Setup configuration of modified Brazilian test; b) elastic stress profile curves for different width of bearing strip.

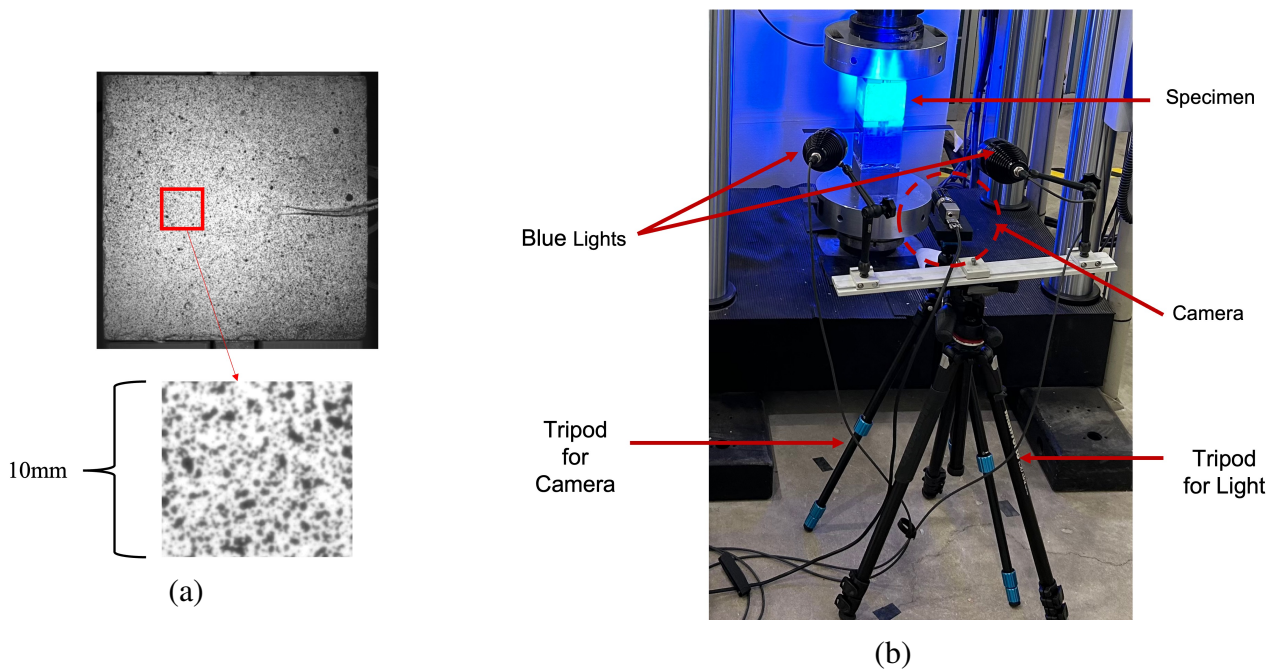


Figure 2: a) Speckles painted face of specimen and speckle size; b) Setup configuration of Aramis for DIC.

hinges on their ability to precisely identify and track small image elements throughout the image sequence. Hence, the quality of the object texture plays a pivotal role in establishing a reliable correspondence between elements in the reference (first) image and the corresponding elements in the deformed ones. To ensure this accuracy, a black-on-white random speckle pattern (Fig. 2a) is carefully applied to each sample's plain face using opaque spray paint. It is crucial to use special DIC-adherent paints that conform to the sample's surface while avoiding the introduction of rigid paint films that may alter the mechanical stress conditions.

The meticulously planned experimental DIC configuration aimed to monitor the indirect tensile tests with both strain gauges and a 2D-DIC system in a simultaneous manner, enabling meaningful comparisons. Throughout the tests, Strain Gauge information was employed, while simultaneously capturing data using Aramis setup. Achieving optimal functioning of the 2D-DIC system necessitates positioning the specimen's surface perpendicular to the camera's axis, which prompts the placement of the Aramis optical module in a front-facing position to enable recording in-plane deformations. GOM's recommended distance to the specimen, varying with the calibration template used (in this case, 290 mm), guides the positioning of the Aramis optical module.

### 2.3.2 DIC Calibration

The selection of camera parameters, encompassing focal length, setup distance, and field of view (FoV), demands careful consideration, as these parameters are intricately interrelated with other intrinsic camera factors such as CCD size. Successfully aligning the desired FoV with the area of interest (AOI) calls for prioritizing the position and setup of the cameras. With a well-considered setup (Fig. 2b), DIC systems adhere to the general recommendation of 2–30 pixels per speckle in the pattern. Furthermore, to ensure adequate brightness and contrast of the pattern, a cold light LED source

is employed. Prior to the experiments, all camera timers are synchronized to facilitate precise adjustments during the post-processing phase. As an additional measure, a digital millisecond timer with its screen within the FoV of the cameras is introduced to verify synchronization.

### 2.3.3 DIC Post-Processing

During the DIC (Digital Image Correlation) process, image acquisition holds utmost significance, and it is crucial to obtain a suitable set of high-quality images to ensure reliable results. To enhance image quality and precision, the GOM software employed an internal protocol based on a calibration plate [1].

This protocol effectively corrected diffraction-related issues, enabling precise adjustment of the aperture size. The result was minimized motion blur and enhanced contrast in the captured images. Throughout the indirect tensile test experiments, images were acquired every second using the Aramis-2D system, ensuring a comprehensive and accurate data collection process. The specimen was loaded until the resulting fracture propagated through the whole specimen from top to bottom and split into 2 halves. The 2D-DIC images were processed with the licensed GOM software, which is capable of computing full-field displacements and strains from a sequence of images [3]. GOM identifies small subsets or regions of interest (ROIs) in the reference image and the deformed image. It then tracks these ROIs through the deformation to find their new positions. Based on the displacements of the ROIs, the software calculates the strain and deformation fields over the entire surface of the object or material. This information provides valuable insights into how the object responds to applied loads or external forces. After obtaining the strain and deformation data, post-processing and visualization are performed to represent the results in a meaningful way. This may include creating contour plots, displacement vectors, strain maps, and other graphical representations [2].

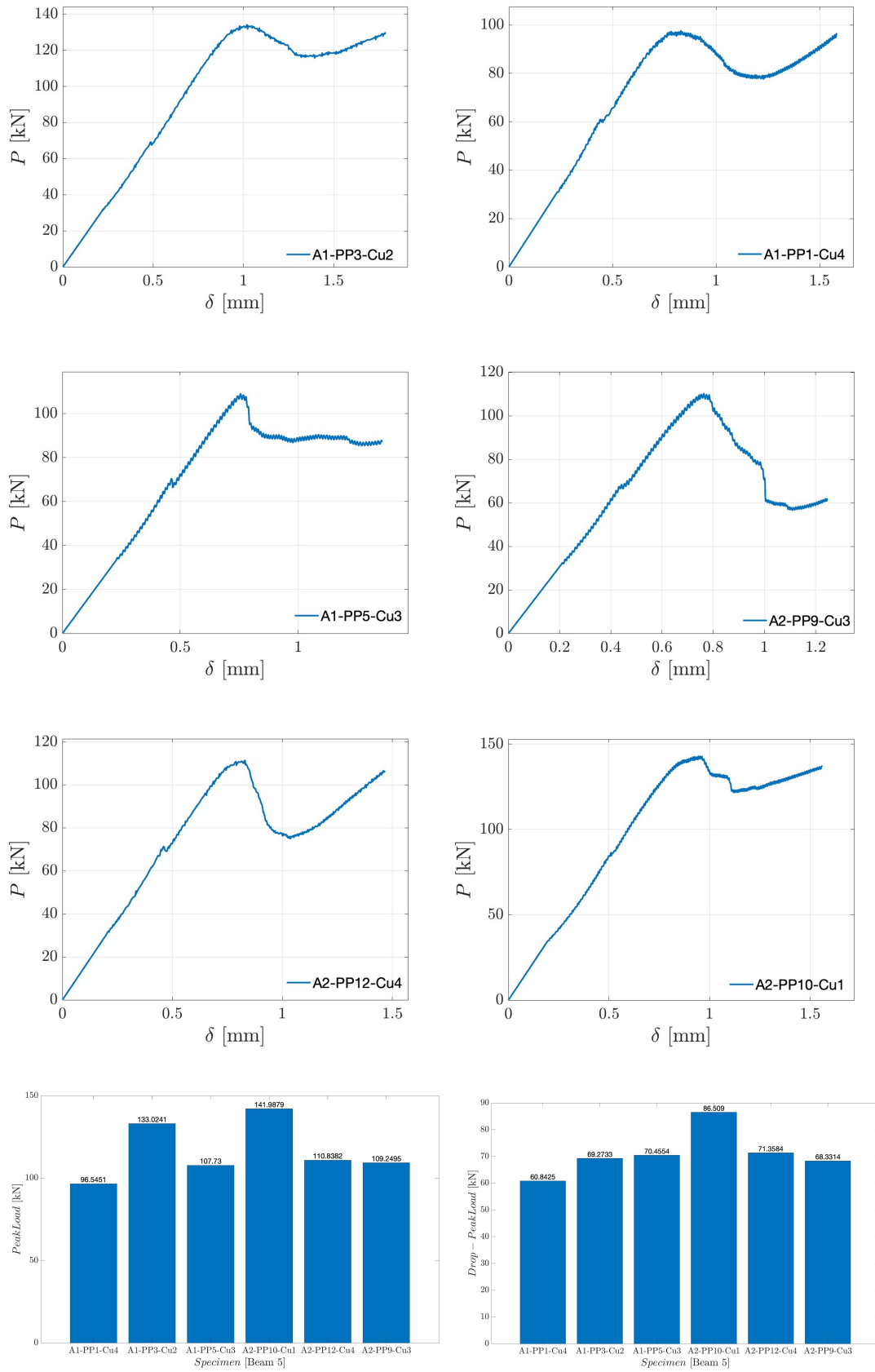


Figure 3: Load vs. displacement curves for six specimen tested, and bargraphs representing peak loads and drop-peak loads.

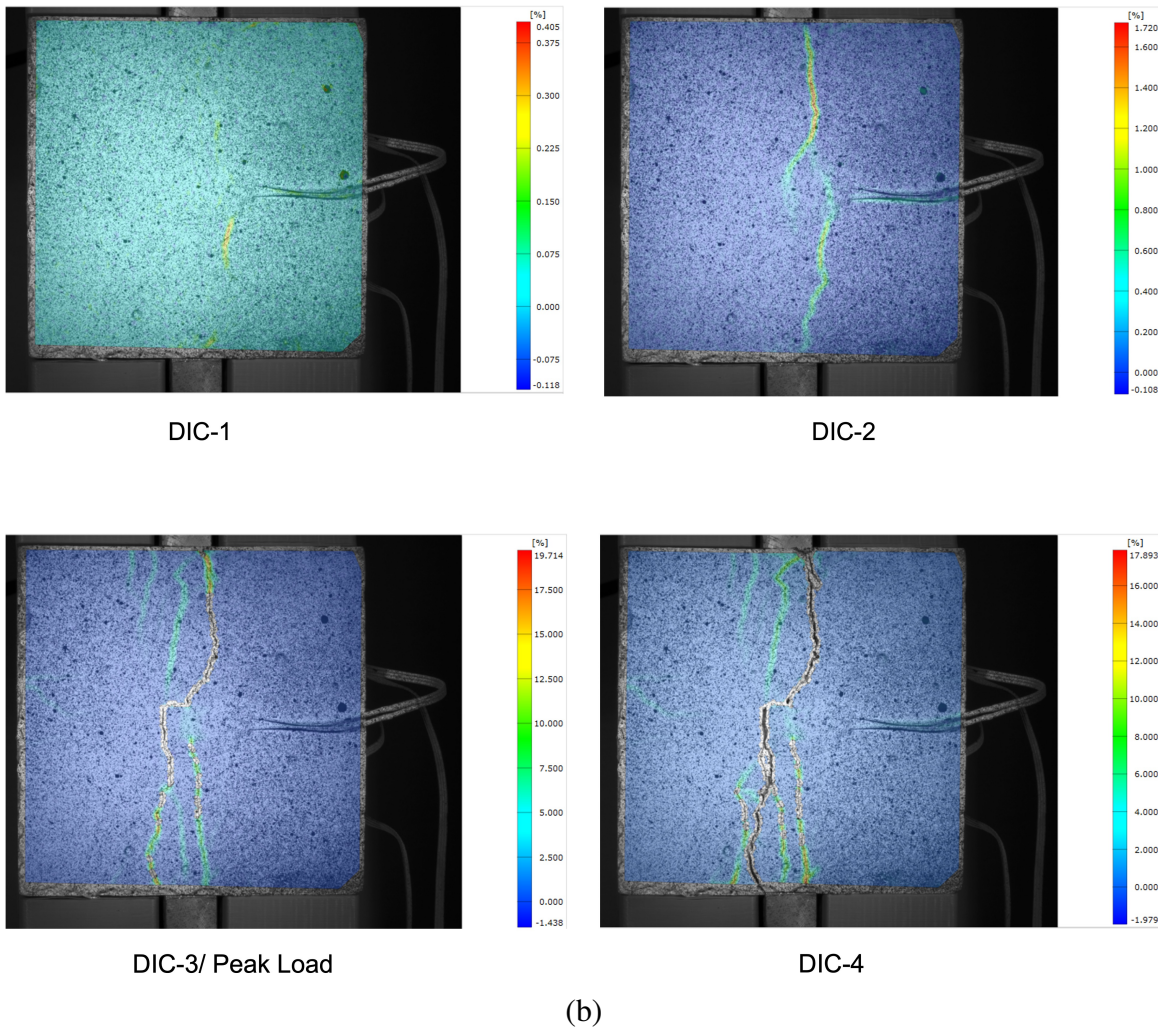
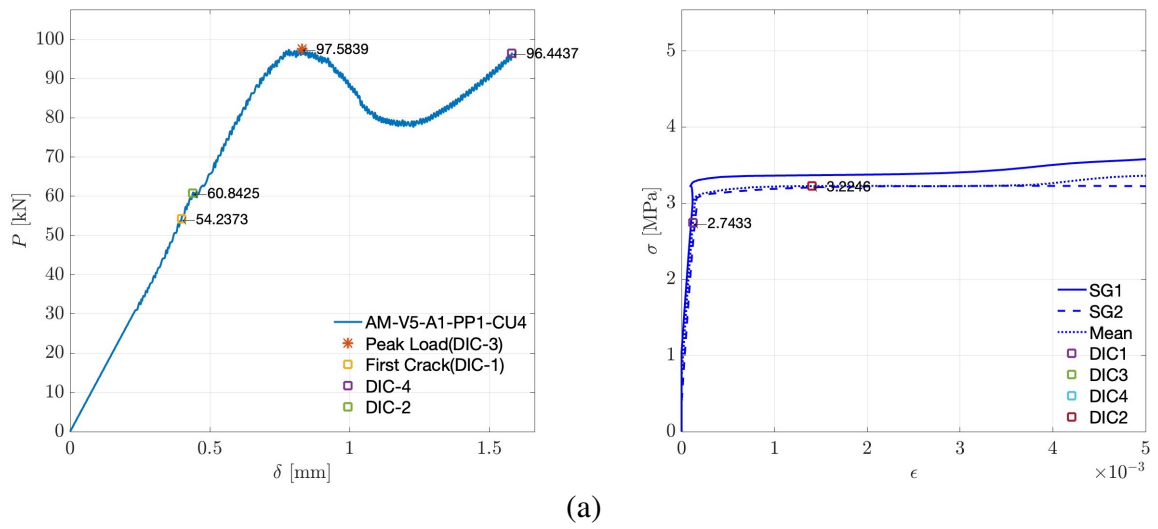


Figure 4: (a) Load vs. displacement ( $P$ - $\delta$ ) and stress vs. strain curves compared with (b) DIC images located on the  $P$ - $\delta$  curve.

### 3 RESULTS AND DISCUSSION

This section presents the results of the failure analysis conducted on SFRC cubes. The outcomes are presented through plots depicting load vs. displacement ( $P$ - $\delta$ ), stress vs. strain ( $\sigma$ - $\epsilon$ , the strain measured using gauges), a comparison of curves with DIC images, and a comparison of peak loads.

Six modified Brazilian tests were carried out in accordance with the procedures outlined in Section 2. The mechanical response of the six specimens are graphically represented in Fig. 3. In all six cases, a drop peak was observed, indicating the onset of a crack in the material's matrix. The peak and drop-peak loads for each case are illustrated in Fig. 3b. Displacement maps were computed from the DIC image dataset captured during each of the six tests.

The experimental findings for SFRC under quasi-static loading were compared with results obtained from DIC and strain gauges. Figure 4a displays the  $P$ - $\delta$  curves for the selected specimens.

#### Crack Initiation Detection

Prior to commencing any analysis on SFRC, it is crucial to address the detection of crack initiation. In this study, the DIC technique was utilized to identify micro-crack initiation and was subsequently compared with the results obtained from strain gauges. Remarkably, in all instances, the surface crack initiation became visible at an approximate magnitude of  $0.4 \mu\text{m}$ . Notably, this observation exhibited a strong correlation with the findings from strain gauges, which were positioned on two faces of the specimen. Furthermore, the appearance of a drop peak in the  $P$ - $\delta$  curve signifies the onset of matrix cracking throughout the section.

The onset of cracking in the matrix is signaled by the drop in load during the pre-peak stage. The drop peak concurs with a rapid increase in strains at the center of the specimen. Figure 4b shows the crack patterns of SFRC under static loading. DIC-1 shows the initiation of cracks and matrix failure, DIC-2 shows fracture propagation through the entire speci-

men from top to bottom, DIC-3 shows the fracture behavior at peak load, and DIC-4 shows the ultimate failure of the specimen. Regarding the corresponding load measurements, the average drop-peak and peak load are 71.1 kN and 116.5 kN respectively, with coefficients of variation of 12% and 15%. Consequently, the drop peak corresponds with a cracking initiation stress in the matrix of 4.5 MPa, whereas the peak load corresponds with an SFRC tensile strength of 7.4 MPa. It bears emphasis that the matrix cracking occurs at 61% of the SFRC tensile strength for this particular material.

### 4 CONCLUSIONS

In this research, the DIC technique was utilized to explore the initiation and propagation of cracks in SFRC and compared it with the conventional strain gauge methodology.

1. The study introduced a modified method for the Brazilian test, enhancing the accuracy and consistency of the findings while aligning with the DIC investigation. Figure 2b illustrates the stress field generated by the selected  $b/L$  ratio.

2. The experimental findings establish the reliability of DIC as a viable alternative to strain gauges. Leveraging the licensed GOM software for image series processing enables the extraction of essential qualitative DIC results, such as major strains, facilitating the observation of local behavioral phenomena during the indirect tensile test.

3. In particular, DIC allows to identify and record the instant for the initiation of a crack in the concrete matrix, which is also detected by the strain gauges and even by a small drop-peak detected by the load cell. For the SFRC used in this research, the cracking of the matrix occurs at only 61% of the tensile strength.

### ACKNOWLEDGEMENTS

The authors gratefully acknowledge the financial support from the *Ministerio de Ciencia e Innovación*, Spain, through grant PID2019-110928RB-C31.

**REFERENCES**

- [1] K Pan, M., CY Rena, G Ruiz., XX Zhang, A De La Rosa, Z Wu (2023) Evolution of the FPZ in steel fiber-reinforced concrete under dynamic mixed-mode loading. *Construction and Building Materials*, 377,1-12
- [2] M Arza-García, C Núñez-Temes, JA Lorenzana, J Ortiz-Sanz, A Castro, M Portela-Barral (2022) Evaluation of a low-cost approach to 2-D digital image correlation vs. a commercial stereo-DIC system in Brazilian testing of soil specimens. *Arch. Civ. Mech. Eng.* 22 (1), 1–13
- [3] Chen L-C, Chang C-Y, Lee W-C, Ma C-C. Full-field measurement of deformation and vibration using digital image correlation. *Smart Sci.* 2015;3:80–6. <https://doi.org/10.1080/23080477.2015.11665640>.
- [4] Peters W, Ranson W (1982) Digital imaging techniques in experimental stress analysis. *Opt Eng* 21(3):213427
- [5] Chu T, Ranson W, Sutton M (1985) Applications of digital-image correlation techniques to experimental mechanics. *Exp-Mech* 25(3): 232–244
- [6] Vendroux G, Knauss W (1998) Submicron deformation field measurements: Part 2. Improved digital image correlation. *Exp Mech* 38(2):86–92
- [7] Bruck HA, McNeill SR, Sutton MA, Peters WH III (1989) Digital image correlation using Newton–Raphson method of partial differential correction. *Exp Mech* 29:261–267
- [8] Cheng P, Sutton MA, Schreier HW, McNeill SR (2002) Full-field speckle pattern image correlation with B-spline deformation function *Exp Mech* 42:344–352
- [9] Kammers AD, Daly S (2011) Small-scale patterning methods for digital image correlation under scanning electron microscopy. *Meas Sci Technol* 22:125501
- [10] Scrivens WA, Luo Y, Sutton MA, Collette SA, Myrick ML, Miney P, Colavita PE, Reynolds AP, Li X (2007) Development of patterns for digital image correlation measurements at reduced length scales. *ExpMech*47(1):6377.[doi:10.1007/s11340-006-5869-y](https://doi.org/10.1007/s11340-006-5869-y)
- [11] Blaber, J.; Antoniou, B.A.B. Ncorr: Open-Source 2D Digital Image Correlation Matlab Software. *Exp. Mech.* 2015, 55, 1105–1122